

Optimal performance of thermoelectric devices with small external irreversibility

Rajeshree Chakraborty* and Ramandeep S. Johal†

Department of Physical Sciences,

Indian Institute of Science Education and Research Mohali,

Sector 81, S.A.S. Nagar,

Manauli PO 140306, Punjab, India.

(Dated: February 12, 2025)

In the thermodynamic analysis of thermoelectric devices, typical irreversibilities are for the processes of finite-rate heat transfer and Joule heating. Approximate analyses often focus on either internal or external irreversibility, yielding well-known expressions for the efficiency at maximum power (EMP), such as the Curzon-Ahlborn value for endoreversible model and the Schmiedl-Seifert form for exoreversible model. Within the Constant Properties model, we formulate a scenario that incorporates internal as well as external irreversibilities simultaneously. We employ the approximation of a symmetric and small external irreversibility (SEI), confining to the regime where the external conductance of the heat exchangers is large in comparison to the internal thermal conductance of the thermoelectric material. This approach allows us to derive a general expression for EMP, which depends on the ratio of internal to external conductance, apart from the figure of merit and ratio of temperatures. Extending our study to thermoelectric refrigerators under the similar assumptions, we also analyze the efficiency at maximum cooling power.

I. INTRODUCTION

A thermoelectric generator (TEG) serves as an paradigmatic model of a realistic heat engine incorporating both internal and external sources of irreversibility [1–3]. The recent global emphasis on energy awareness has underscored the importance of unconventional methods for generating electrical energy. TEGs, which leverage the Seebeck effect, are eco-friendly in this respect [4, 5]. They have garnered increasing attention due to such advantages as minimal noise, zero emissions and extended operational life [6]. Low-temperature TEGs are particularly versatile, finding applications in diverse areas where waste heat is prevalent, such as industrial engineering [7], photovoltaic generation [8, 9], aviation [10], electronic devices [11], and internal combustion engines [12]. In recent years, considerable efforts have been made to identify thermoelectric materials with enhanced performance [13, 14]. In addition to improving the figure of merit [15–20], the system analysis and optimization of a TEG are crucial for developing high-

* e-mail: mp18011@iisermohali.ac.in

† e-mail: rsjohal@iisermohali.ac.in

performance thermoelectric systems [21–29]. In this quest, a prevalent optimization technique adopted for TEG is the power output maximization, with an associated interesting parameter known as the efficiency at maximum power (EMP) [30–33].

In the context of finite-time thermodynamics, Curzon-Ahlborn efficiency given by $\eta_{CA} = 1 - \sqrt{T_c/T_h}$ is significant, where T_h and T_c being the temperatures of the hot and cold reservoirs, respectively. This expression for EMP was derived for a specific class of heat engines known as endoreversible heat engines [34–36] which assume that irreversibilities arise solely from finite heat transfer rates between the working substance and the heat reservoirs. A different expression for EMP was later derived for the so-called exoreversible heat engines, which attribute irreversibilities to internal dissipations, such as friction and Joule heating, while assuming perfect thermal contacts. Schmiedl and Seifert [37] derived this efficiency as $\eta_{SS} = \eta_C/(2 - \gamma\eta_C)$, where γ ranges from 0 to 1 and takes the value 1/2 for homogeneous thermoelectric materials, indicating symmetric Joule heat dissipation in both hot and cold reservoirs [38]. Kaur and Johal [39] conducted a study on the optimal power of TEG with both internal and external irreversibilities characterized by a spatially dependent internal thermal conductivity which leads to asymmetric dumping of Joule heat on the hot and cold sides. The inhomogeneity of internal thermal conductivity was shown to enhance the performance of TEG-coupled hybrid systems such as the molten carbonate fuel cell [40] and the evacuated U-tube solar collector [41]. The effect of space-dependent electrical conductivity in a thermoelectric cooler was also studied recently [42, 43].

The previous research on the optimization of TEGs indicates that a comprehensive and predictive thermodynamic model incorporating both internal and external irreversibilities, is considered intractable i.e. the model cannot be solved analytically without introducing certain approximations. Indeed, a solvable model is crucial for gaining insight into operational regimes and a suitable device design. The present work analyzes the Constant Properties (CP) model by including internal irreversibilities and finite rates of heat transfer on both hot and cold contacts—under the approximation of a small external irreversibility (SEI). Optimizing the power output, we derive a compact general expression for EMP that depends on three quantities: i) the ratio of cold to hot temperatures, ii) the figure of merit of the thermoelectric material and iii) the ratio of internal to external thermal conductances. Different performance bounds are analyzed while recovering the known cases of endoreversible and exoreversible approximations. We also study thermoelectric refrigerators (TER) under the SEI approximation, where the focus is on the optimization of cooling power and to analyze the efficiency at maximum cooling power (EMCP). The bounds derived from this expression not only reveal the system’s convergence to the well-established exoreversible model of TER [44], but also extend the previous analysis.

Our paper is structured as follows. Section II details the model of a thermoelectric generator where

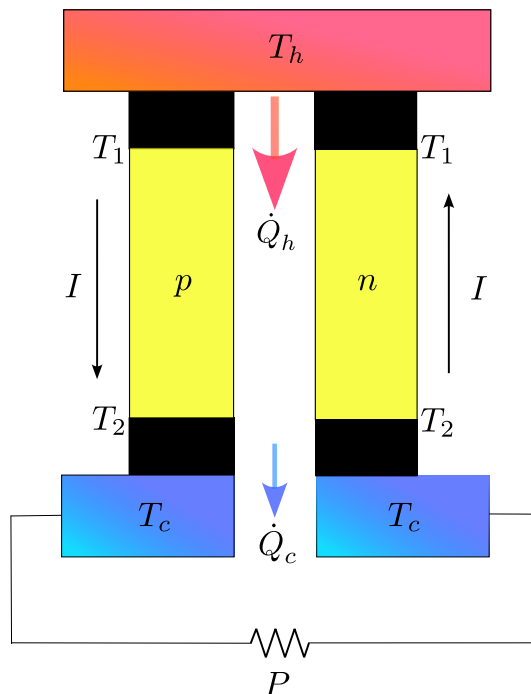


FIG. 1. Schematic representation of a two-leg thermoelectric generator (TEG), illustrating the heat source and the sink, the flow of heat and the extraction of electrical power via an external load. p - and n -type each represents a TEM, while the hatched segments are heat exchangers with symmetric thermal conductance K on hot and cold sides.

in Section II.A we present the case of SEI and optimize the power output. In Section II.B the properties of EMP are analyzed in some detail. In Section II.C, we make comparison of our model with the exact model using the experimental data on thermoelectric materials. In Section III, we present the model for a thermoelectric refrigerator and address the optimization of cooling power. Section IV concludes with a summary and final remarks.

II. THERMOELECTRIC GENERATOR MODEL

We consider a specific design for the two-leg configuration of TEG as shown in Fig. 1. The materials in n -type and p -type legs have electrical resistivities, ρ_n and ρ_p , thermal conductivities k_n and k_p , and Seebeck coefficients α_n and α_p , respectively. The thermoelectric material (TEM) is regarded as a homogeneous one-dimensional substance of length L , with internal resistance R , heat transfer conductance K_0 and Seebeck coefficient, $\alpha = \alpha_p - \alpha_n$ [45], within the CP model [1]. K_h and K_c represent the thermal conductances of the heat exchangers that connect the TEM to the heat source on the hot side and the heat sink on the cold side, respectively. For convenience, we consider the symmetric case, $K_h = K_c \equiv K$, with a small external irreversibility (SEI) i.e. K is large but finite. It will be seen below, that operation

of TEG requires that K_0 be small compared to K .

Let I denote the constant value of the electric current flowing through the TEG. On the basis of the Onsager formalism and Domenicali's heat equation [45, 46], the thermal currents at the hot and cold contacts of the TEM can be respectively written as

$$\dot{Q}_h = \alpha T_1 I + K_0(T_1 - T_2) - \frac{1}{2} R I^2, \quad (1)$$

$$\dot{Q}_c = \alpha T_2 I + K_0(T_1 - T_2) + \frac{1}{2} R I^2, \quad (2)$$

where T_1, T_2 are the local temperatures at the junction of TEM and heat exchangers, such that $T_1 < T_h$ ($T_2 > T_c$) (see Fig. 1). The first term in the above equations corresponds to convective heat flow. The second term denotes the heat leakage across the TEM, while the last term accounts for the Joule heating effect as derived within the CP model. We consider the heat transfer law through the heat exchangers to be Newtonian so that the thermal currents at the hot and cold junctions can be written as

$$\dot{Q}_h = K(T_h - T_1), \quad (3)$$

$$\dot{Q}_c = K(T_2 - T_c), \quad (4)$$

respectively. In the limit when the thermal contacts between the reservoirs and TEM are ideal ($K \rightarrow \infty$), we have $T_1 \rightarrow T_h$ and $T_2 \rightarrow T_c$, and the flux equations are simplified to:

$$\dot{Q}_h = \alpha T_h I + K_0(T_h - T_c) - \frac{1}{2} R I^2, \quad (5)$$

$$\dot{Q}_c = \alpha T_c I + K_0(T_h - T_c) + \frac{1}{2} R I^2. \quad (6)$$

For the non-ideal thermal contacts, the flux-matching conditions equate Eqs. (1) and (3) (similarly Eq. (2) equals (4)), so that we can explicitly solve for T_1 and T_2 :

$$T_1 = \frac{2K\alpha T_h I + (K + 2K_0)R I^2 + \alpha R I^3 + 2K(KT_h + K_0(T_c + T_h))}{2[K(K + 2K_0) - \alpha^2 I^2]}, \quad (7)$$

$$T_2 = \frac{2K\alpha T_c I + (K + 2K_0)R I^2 + \alpha R I^3 + 2K(KT_c + K_0(T_c + T_h))}{2[K(K + 2K_0) - \alpha^2 I^2]}. \quad (8)$$

Substituting these expressions back into Eqs. (1) and (2), we can obtain explicit expressions for the hot and the cold fluxes. Then, the power output ($P = \dot{Q}_h - \dot{Q}_c$) is obtained in the form:

$$P = \frac{\alpha(T_h - T_c) K^2 I - K(K + 2K_0) R I^2 - \alpha^2(T_c + T_h) K I^2}{K(K + 2K_0) - \alpha^2 I^2}. \quad (9)$$

However, the solution for the optimal power from the above expression hardly provides an insight. Various approximations have been considered in literature, such as endoreversible approximation which treats R and K_0 to be negligible, or the exoreversible approximation which implies $K \rightarrow \infty$ limit. These studies

aim to exclude either internal or the external irreversibility. The so-called strong-coupling approximation which neglects K_0 is also artificial since in dealing with real materials, it is difficult to reduce K_0 without increasing R , a stumbling block towards achieving a high figure of merit [Eq. (13)]. In this paper, we formulate our model with both the internal and external irreversibilities, however, with the simplification that the latter irreversibility is assumed to be small (as qualified below) as well as symmetric on the two sides.

A. Regime of small external irreversibility (SEI)

Now, keeping terms up to first order in the small parameter $1/K$, the thermal flux equations (leading to Eq. (9)) can be written in an approximate form as:

$$\dot{Q}_h = \left(1 - \frac{2K_0}{K}\right) [\alpha T_h I + K_0(T_h - T_c)] - \left(\frac{R}{2} + \frac{\alpha^2 T_h}{K}\right) I^2 + \frac{\alpha R}{2K} I^3, \quad (10)$$

$$\dot{Q}_c = \left(1 - \frac{2K_0}{K}\right) [\alpha T_c I + K_0(T_h - T_c)] + \left(\frac{R}{2} + \frac{\alpha^2 T_c}{K}\right) I^2 + \frac{\alpha R}{2K} I^3. \quad (11)$$

The expression of power output is given by

$$P = \left(1 - \frac{2K_0}{K}\right) \alpha (T_h - T_c) I - \left(R + \frac{\alpha^2}{K} (T_h + T_c)\right) I^2, \quad (12)$$

where the cubic terms in I cancel out, retaining a quadratic expression for the power output. Since the thermal fluxes still contain the cubic term, the present model is beyond the linear-irreversible regime [3]. The performance of a thermoelectric device is usually characterized by the figure of merit of TEM, defined as

$$z = \frac{\alpha^2 T_h}{RK_0}. \quad (13)$$

In the case of SEI, apart from the parameter z , the performance also depends on the parameter

$$k = \frac{K_0}{K}. \quad (14)$$

For instance, the positivity of power in Eq. (12) requires that $k < 1/2$.

Now, the power output vanishes when $I = 0$, as well as in the short-circuit (sc) limit, given by

$$I_{\text{sc}} = \frac{\alpha(T_h - T_c)}{R} \frac{(1 - 2k)}{1 + kz(2 - \eta_C)}. \quad (15)$$

For a given TEM with a finite z value, as $k \rightarrow 0$ (implying $K \gg K_0$), the maximum current reduces to: $i_{\text{sc}} = \alpha(T_h - T_c)/R$ [2]. Clearly, the regime of a non-zero power output shrinks (since $I_{\text{sc}} < i_{\text{sc}}$) in

the presence of external irreversibility. Now, optimizing P with respect to I in the interval $[0, I_{sc}]$, the optimal current is $I^* = I_{sc}/2$. The expression for optimal power is given by

$$P^* = \frac{\alpha^2(1-2k)^2 T_h^2 \eta_C^2}{4R [1 + kz(2 - \eta_C)]}. \quad (16)$$

In $k \rightarrow 0$ limit, we obtain $P^* = \alpha^2 T_h^2 \eta_C^2 / 4R$ [2]. Further, the difference in the junction temperatures, at the optimal power, is given by:

$$T_1^* - T_2^* = (T_h - T_c) \left(1 - k \left[z + 2 - \frac{z\eta_C}{2} \right] \right). \quad (17)$$

As expected, for $k \rightarrow 0$, the temperature difference between the ends of TEM approaches the difference in reservoir temperatures.

B. Efficiency at maximum power (EMP)

EMP is an important quantifier to study of the performance of a finite-time engine. Defined as the ratio of the optimal power output (P^*) to the corresponding hot flux ($\dot{Q}_h(I^*)$), the EMP of our model can be compactly written as

$$\eta^* = \frac{A}{B}, \quad (18)$$

where we denote

$$\begin{aligned} A &= 4(1-2k)(2kz+1-kz\eta_C)^2, \\ B &= [4k(-4kz\eta_C+18kz+k+3z+10)+3]kz\eta_C-2(2kz+1)[2(14k+5)kz+22k+1] \\ &\quad + \frac{8}{z\eta_C}(2kz+1)^2(2kz+z+2), \end{aligned}$$

which is expressed only in terms of the parameters z , η_C and k . The above closed form expression for EMP quantifies the influence of both internal and external irreversibilities in a TEG. The known cases of only internal (or external) irreversibility may be obtained from the above expression. For a finite z value, we obtain

$$\lim_{k \rightarrow 0} \eta^* = \frac{2z\eta_C}{8+z(4-\eta_C)}. \quad (19)$$

This expression is bounded from above by the large- z limit. These two limits may be compactly depicted as:

$$\lim_{z \rightarrow \infty} \lim_{k \rightarrow 0} \eta^* = \frac{2\eta_C}{4-\eta_C}, \quad (20)$$

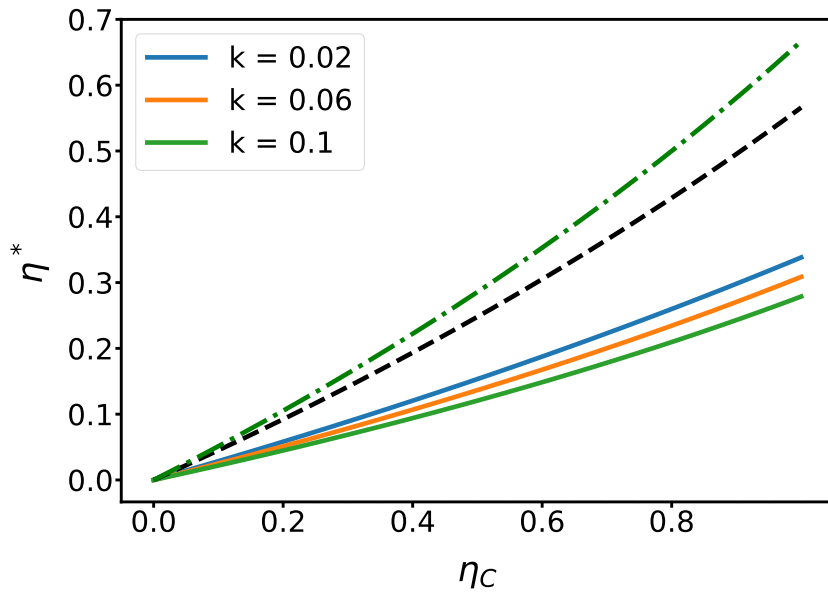


FIG. 2. Efficiency at maximum power (EMP), Eq. (18), at a given $k < 1/2$ vs. Carnot efficiency (η_C) for $z = 3$. With k decreasing from bottom upwards, the EMP approaches the black dashed curve in the limit $k \rightarrow 0$, given by Eq. (19). The top dot-dashed curve, given by Eq. (20), is approached in the ideal limit $z \rightarrow \infty$.

which is η_{SS} for the symmetric case ($\gamma = 1/2$) in the exoreversible approximation. These limits are depicted in Fig. 2.

On the other hand, first taking the $z \rightarrow \infty$ limit for a finite k , followed by $k \rightarrow 0$, we obtain

$$\lim_{k \rightarrow 0} \lim_{z \rightarrow \infty} \eta^* = \frac{2 - \eta_C}{4 - 3\eta_C} \eta_C. \quad (21)$$

The above form for EMP is obtained in coupled linear-irreversible engines [47] and Feynman's ratchet in the hot temperatures limit [48]. Thus, we note that the limits of a vanishing- k and a diverging- z do not commute with each other. Actually, Eq. (21) yields a higher value of EMP than Eq. (20). In view of the fact that the real thermoelectric materials have a finite value of z , η_{SS} may be the more relevant bound for TEGs.

To gain more insight into the general expression for EMP, we consider small temperature difference or $\eta_C \ll 1$, whereby EMP can be expressed in series form as:

$$\eta^* = \frac{(1 - 2k)z}{2(2kz + z + 2)} \eta_C + \frac{(4k(1 - 3k) + 1)z^2}{8(2kz + z + 2)^2} \eta_C^2 + \mathcal{O}(\eta_C^3). \quad (22)$$

For finite z and $k \rightarrow 0$ [Eq. (19)], the series is simplified as follows.

$$\eta^* = \frac{z}{2(z + 2)} \eta_C + \frac{z^2}{8(z + 2)^2} \eta_C^2 + \mathcal{O}(\eta_C^3). \quad (23)$$

Further, in the limit of large z , we obtain universal terms in the series for EMP:

$$\eta^* = \frac{\eta_C}{2} + \frac{\eta_C^2}{8} + \mathcal{O}(\eta_C^3). \quad (24)$$

Interestingly, the same expansion is obtained up to the quadratic term if we reverse the order of the two limits. This shows an underlying aspect of the universality of EMP beyond the linear response regime, which is independent of the way the limit is approached. In general, the factor 1/2 in the linear term [Eq. (24)] represents the upper bound of EMP in the linear response regime [30] while the 1/8 factor in the quadratic term may be related to a certain left-right symmetry in the system [31].

C. Comparison of the model

We have compared the SEI model with the exact model using experimental values for the various parameters, as extracted from Ref. [49] and given in Table I. In Fig. 3, parametric loop curves are drawn between the power output and the corresponding efficiency. The SEI model shows similar trend as far as the general shape of the curves is concerned. The area enclosed by the loops increases as the temperature gradient increases, thus increasing both the maximum power and the maximum efficiency. We expect a better agreement of SEI model with the exact model for smaller k values which is apparent in Fig. 3.

Case	T_h (K)	T_c (K)	$\eta_C = 1 - \frac{T_c}{T_h}$	K_0 (W m ⁻² K ⁻¹)	α (V K ⁻¹)	R (Ω)	$z = \frac{\alpha^2 T_h}{R K_0}$
1	384	324	0.16	8.6×10^{-3}	5.0×10^{-4}	7.7×10^{-3}	1.45
2	413	333	0.19	8.8×10^{-3}	5.0×10^{-4}	8.5×10^{-3}	1.38
3	444	342	0.23	9.0×10^{-3}	5.1×10^{-4}	9.2×10^{-3}	1.4
4	498	348	0.30	10.0×10^{-3}	5.0×10^{-4}	9.9×10^{-3}	1.26

TABLE I. Parameters for TEG used in Fig. 3 and based on Ref. [49].

III. THERMOELECTRIC REFRIGERATOR (TER)

We now study the optimal performance of a TER within the regime of SEI. Fig. 4 presents a schematic of the TER showing the various fluxes and temperatures. Heat flux from the cold reservoir is pushed against the temperature gradient using the external electric power, due to thermoelectric effect. Note that for TER, $T_1 > T_h$ and $T_2 < T_c$. Our target function here is the cold flux \dot{Q}_c , also known as the cooling power. It has been noted [44] that an endoreversible model of TER does not yield an optimum cooling power unlike the exoreversible model. Here, we investigate the effect of both external and internal irreversibilities in the regime of SEI. Within the CP model for a TER, the thermal fluxes are given by

$$\dot{Q}_h = \alpha T_1 I - K_0(T_1 - T_2) + \frac{1}{2} R I^2, \quad (25)$$

$$\dot{Q}_c = \alpha T_2 I - K_0(T_1 - T_2) - \frac{1}{2} R I^2. \quad (26)$$

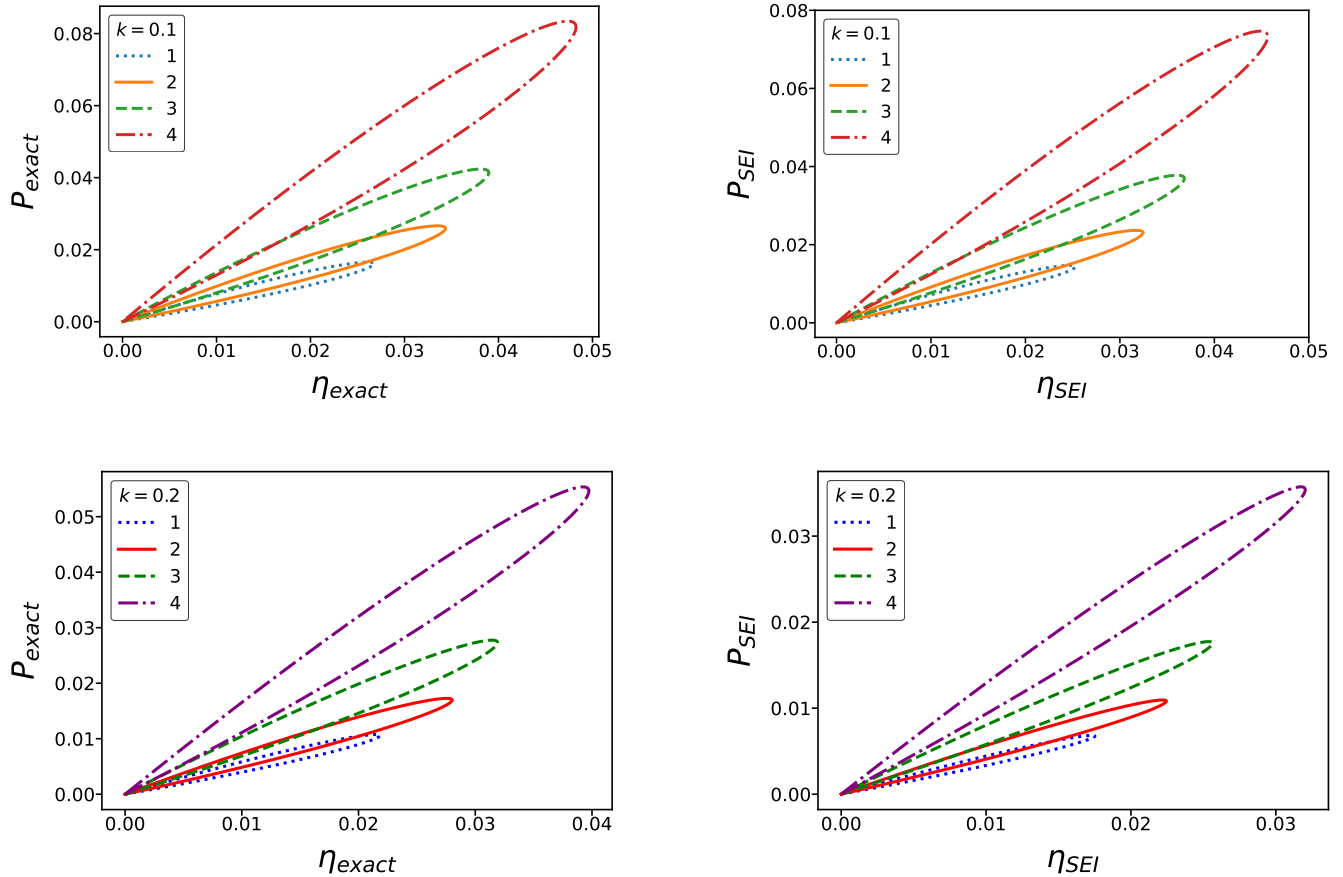


FIG. 3. Power output versus efficiency for the exact and the SEI models with $k = 0.1$ (top left and right) and $k = 0.2$ (bottom left and right). Legends 1, 2, 3 and 4 correspond to the data for the specific curve as listed in Table I.

Assuming that the thermal flux through a heat exchanger is Newtonian, the thermal currents at the junctions are

$$\dot{Q}_h = K(T_1 - T_h), \quad (27)$$

$$\dot{Q}_c = -K(T_2 - T_c). \quad (28)$$

From the above set of equations, we can find here the explicit expressions for T_1 and T_2 , similar to the case of TEG. Upon substituting these into Eq. (25) and (26), we obtain the final heat flux equations.

A. Regime of SEI

In the large- K approximation, we truncate the final expressions for the heat fluxes keeping terms in $1/K$, and obtain

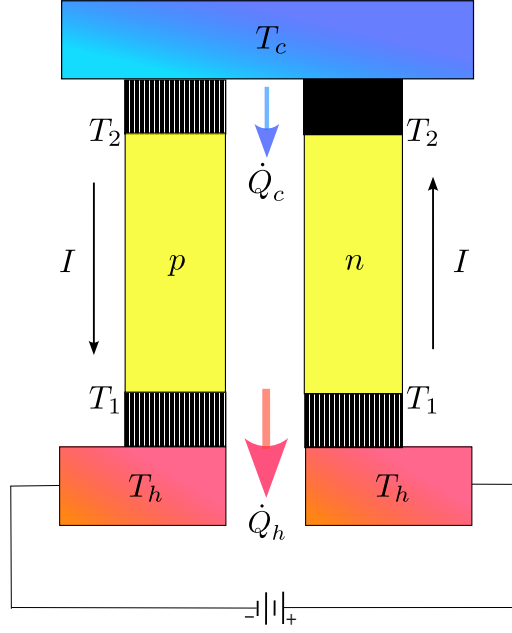


FIG. 4. Schematic of a two-leg thermoelectric refrigerator, highlighting the key components such as the thermoelectric module, thermal contacts, heat fluxes and the power source.

$$\dot{Q}_h = \left(1 - \frac{2K_0}{K}\right) [\alpha T_h I - K_0(T_h - T_c)] + \left(\frac{R}{2} + \frac{\alpha^2 T_h}{K}\right) I^2 + \frac{\alpha R}{2K} I^3, \quad (29)$$

$$\dot{Q}_c = \left(1 - \frac{2K_0}{K}\right) [\alpha T_c I - K_0(T_h - T_c)] - \left(\frac{R}{2} + \frac{\alpha^2 T_c}{K}\right) I^2 + \frac{\alpha R}{2K} I^3. \quad (30)$$

The power input ($P = \dot{Q}_h - \dot{Q}_c$) is given by

$$P = \left(1 - \frac{2K_0}{K}\right) \alpha (T_h - T_c) I + \left(R + \frac{\alpha^2}{K} (T_h + T_c)\right) I^2. \quad (31)$$

To optimize the cooling power [Eq. (30)], we set $(\partial/\partial I)\dot{Q}_c = 0$. The optimal input current is

$$I^* = \frac{K_0}{3\alpha k} (1 + 2kz - \sqrt{1 - 2kz(1 - 2k(3 + z))}), \quad (32)$$

where we define the figure of merit in the refrigerator mode as

$$z = \frac{\alpha^2 T_c}{RK_0}. \quad (33)$$

The condition $I^* > 0$ requires that $k < 1/2$. The condition of maximum, $(\partial/\partial I)^2 \dot{Q}_c|_{I=I^*} < 0$ is also verified. For a given TEM, the limit $k = K_0/K \rightarrow 0$ yields $I^* = \alpha T_c/R$. Likewise, the optimal cooling power is given by:

$$\lim_{k \rightarrow 0} \dot{Q}_c^* = K_0 T_c \left(\frac{z}{2} - \frac{1}{\epsilon C} \right), \quad (34)$$

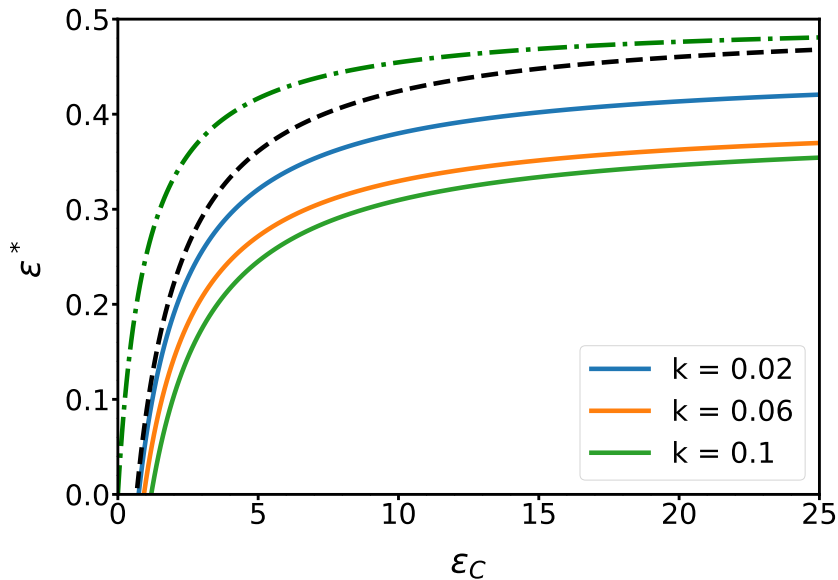


FIG. 5. EMCP at given k values vs. ϵ_C . As k vanishes from bottom upwards, the EMCP approaches the dashed curve in the limit $k \rightarrow 0$, given by Eq. (35). $z = 3$ is chosen in this figure. The top dot-dashed curve, given by $\epsilon_C/2(1 + \epsilon_C)$, is reached for $z \rightarrow \infty$.

where $\epsilon_C = T_c/(T_h - T_c)$ defines the coefficient of performance of a Carnot refrigerator. Thus, the optimal cooling power condition requires that $z > 2/\epsilon_C$ if the external thermal contacts are regarded as reversible. The corresponding efficiency at maximum cooling power (EMCP), defined as $\epsilon^* = \dot{Q}_c^*/P(I^*)$, is given by:

$$\lim_{k \rightarrow 0} \epsilon^* = \frac{z\epsilon_C - 2}{2z(1 + \epsilon_C)}. \quad (35)$$

For large- z values, it reduces monotonically to the expression $\epsilon_C/2(1 + \epsilon_C)$, which is also the EMCP in exoreversible limit [44]. The general formula for EMCP in the present approximation ($0 < k < 1/2$) depends in a complicated way on k , z and ϵ_C , which we do not present here for the sake of brevity and depict graphically in Fig. 5.

IV. CONCLUSIONS

In this work, we studied the optimum performance of thermoelectric devices with an analytic model incorporating both internal and external irreversibilities. While the real thermoelectric materials have a finite figure of merit leading to internal irreversibilities in the form of heat leak and Joule heating, the external irreversibilities owing to finite thermal conductance of the heat exchangers also decrease the performance of the devices. Within the Constant Properties model, we make two further assumptions in order to facilitate a tractable solution: i) a small external irreversibility and ii) equal thermal conductance of heat exchangers at the hot and cold junctions. An advantage of this simplification is that the power

output of a TEG is still a quadratic function of the electric current, similar to the case of no external irreversibility. However, the heat fluxes depend cubically on the current, which implies that the model is beyond the linear-irreversible regime. We derived a general expression for the efficiency at maximum power which is shown to depend upon the ratio (k) of internal to external thermal conductance, apart from the ratio of temperatures and the figure of merit. The SEI model yields the operation of an engine only in the regime $k < 1/2$.

Similarly, we have extended the analysis to thermoelectric refrigerators where the efficiency at maximum cooling power is shown to depend on the Carnot coefficient, the figure of merit and the ratio k . The condition $k < 1/2$ is also relevant in the case of the TER model. Earlier studies showed that the cooling power is optimizable only for the exoreversible model. Our analysis extends it into the regime of small external irreversibility. In the present model, the limit of a vanishing external irreversibility can be looked upon as the smallness of K_0 in comparison with K ($K_0 \ll K$). It is hoped that the SEI model may provide practical indicators to benchmark the performance of thermoelectric devices where the heat exchangers' thermal conductance is much larger than the thermoelectric material. The present study thus bridges the gap between simpler, idealized models (like endoreversible and exoreversible ones) and realistic thermoelectric devices, offering an insight into the interplay between external and internal irreversibilities which may guide their practical design.

ACKNOWLEDGMENTS

RC acknowledges gratitude to Indian Institute of Science Education and Research Mohali for the grant of research fellowship.

-
- [1] A. F. Ioffe, *Semiconductor Thermoelements and Thermoelectric Cooling* (Infosearch, 1958).
 - [2] J. Gordon, Generalized power versus efficiency characteristics of heat engines: The thermoelectric generator as an instructive illustration, *American Journal of Physics* **59**, 551 (1991).
 - [3] Y. Apertet, H. Ouerdane, C. Goupil, and P. Lecoeur, Irreversibilities and efficiency at maximum power of heat engines: The illustrative case of a thermoelectric generator, *Physical Review E* **85**, 031116 (2012).
 - [4] F. J. DiSalvo, Thermoelectric cooling and power generation, *Science* **285**, 703 (1999).
 - [5] D. M. Rowe, *Thermoelectrics handbook: Macro to Nano* (CRC press, 2018).
 - [6] M. Gomez, B. Ohara, R. Reid, and H. Lee, Investigation of the effect of electrical current variance on thermoelectric energy harvesting, *Journal of electronic materials* **43**, 1744 (2014).
 - [7] Z. Miao, X. Meng, and L. Liu, Industrial experiment and numerical analysis of the effect of pulsing water flow in thermoelectric generators, *Applied Thermal Engineering* **226**, 120285 (2023).

- [8] R. Lamba and S. C. Kaushik, Modeling and performance analysis of a concentrated photovoltaic–thermoelectric hybrid power generation system, *Energy Conversion and Management* **115**, 288 (2016).
- [9] A. Yusuf and S. Ballikaya, Exergetic assessment of a concentrated photovoltaic-thermoelectric system with consideration of contact resistance, *International Journal of Exergy* **38**, 411 (2022).
- [10] D. Samson, T. Otterpohl, M. Kluge, U. Schmid, and T. Becker, Aircraft-specific thermoelectric generator module, *Journal of Electronic Materials* **39**, 2092 (2010).
- [11] M. Barrubeeah, M. Rady, A. Attar, F. Albatati, and A. Abuhabaya, Design, modeling and parametric optimization of thermoelectric cooling systems for high power density electronic devices, *International Journal of Low-Carbon Technologies* **16**, 1060 (2021).
- [12] P. Fernández-Yáñez, O. Armas, R. Kiwan, A. Stefanopoulou, and A. Boehman, A thermoelectric generator in exhaust systems of spark-ignition and compression-ignition engines. a comparison with an electric turbo-generator, *Applied Energy* **229**, 80 (2018).
- [13] B. Poudel, Q. Hao, Y. Ma, Y. Lan, A. Minnich, B. Yu, X. Yan, D. Wang, A. Muto, D. Vashaee, *et al.*, High-thermoelectric performance of nanostructured Bismuth Antimony Telluride bulk alloys, *Science* **320**, 634 (2008).
- [14] D.-Y. Chung, T. Hogan, P. Brazis, M. Rocci-Lane, C. Kannewurf, M. Bastea, C. Uher, and M. G. Kanatzidis, CsBi₄Te₆: A high-performance thermoelectric material for low-temperature applications, *Science* **287**, 1024 (2000).
- [15] D. Nemir and J. Beck, On the significance of the thermoelectric figure of merit z , *Journal of electronic materials* **39**, 1897 (2010).
- [16] H. Littman and B. Davidson, Theoretical bound on the thermoelectric figure of merit from irreversible thermodynamics, *Journal of Applied Physics* **32**, 217 (1961).
- [17] A. Majumdar, Thermoelectricity in semiconductor nanostructures, *Science* **303**, 777 (2004).
- [18] A. Shakouri, Recent developments in semiconductor thermoelectric physics and materials, *Annual Review of Materials Research* **41**, 399 (2011).
- [19] B. Muralidharan and M. Grifoni, Performance analysis of an interacting quantum dot thermoelectric setup, *Phys. Rev. B* **85**, 155423 (2012).
- [20] Y. Feng, L. Chen, F. Meng, and F. Sun, Thermodynamic analysis of TEG-TEC device including influence of Thomson effect, *Journal of Non-Equilibrium Thermodynamics* **43**, 75 (2018).
- [21] G. J. Snyder and T. S. Ursell, Thermoelectric efficiency and compatibility, *Physical Review Letters* **91**, 148301 (2003).
- [22] I. Iyyappan and M. Ponmurugan, Thermoelectric energy converters under a trade-off figure of merit with broken time-reversal symmetry, *Journal of Statistical Mechanics: Theory and Experiment* **2017**, 093207 (2017).
- [23] S. B. Riffat and X. Ma, Thermoelectrics: a review of present and potential applications, *Applied thermal engineering* **23**, 913 (2003).
- [24] Y. Pei, X. Shi, A. LaLonde, H. Wang, L. Chen, and G. J. Snyder, Convergence of electronic bands for high performance bulk thermoelectrics, *Nature* **473**, 66 (2011).

- [25] C. Goupil, W. Seifert, K. Zabrocki, E. Müller, and G. J. Snyder, Thermodynamics of thermoelectric phenomena and applications, *Entropy* **13**, 1481 (2011).
- [26] H. J. Goldsmid *et al.*, *Introduction to thermoelectricity*, Vol. 121 (Springer, 2010).
- [27] J.-H. Meng, X.-X. Zhang, and X.-D. Wang, Multi-objective and multi-parameter optimization of a thermoelectric generator module, *Energy* **71**, 367 (2014).
- [28] W.-H. Chen, S.-R. Huang, and Y.-L. Lin, Performance analysis and optimum operation of a thermoelectric generator by taguchi method, *Applied Energy* **158**, 44 (2015).
- [29] R. Lamba, S. Manikandan, S. C. Kaushik, and S. K. Tyagi, Thermodynamic modelling and performance optimization of trapezoidal thermoelectric cooler using genetic algorithm, *Thermal Science and Engineering Progress* **6**, 236 (2018).
- [30] C. Van den Broeck, Thermodynamic efficiency at maximum power, *Physical Review Letters* **95**, 190602 (2005).
- [31] M. Esposito, K. Lindenberg, and C. Van den Broeck, Universality of efficiency at maximum power, *Physical Review Letters* **102**, 130602 (2009).
- [32] H. Ouerdane, Y. Apertet, C. Goupil, and P. Lecoeur, Continuity and boundary conditions in thermodynamics: From Carnot's efficiency to efficiencies at maximum power, *The European Physical Journal Special Topics* **224**, 839 (2015).
- [33] M. Moreau, B. Gaveau, and L. Schulman, Efficiency of a thermodynamic motor at maximum power, *Physical Review E—Statistical, Nonlinear, and Soft Matter Physics* **85**, 021129 (2012).
- [34] I. I. Novikov, The efficiency of atomic power stations (a review), *Journal of Nuclear Energy (1954)* **7**, 125 (1958).
- [35] F. L. Curzon and B. Ahlborn, Efficiency of a Carnot engine at maximum power output, *American Journal of Physics* **43**, 22 (1975).
- [36] D. Agrawal and V. Menon, The thermoelectric generator as an endoreversible Carnot engine, *Journal of Physics D: Applied Physics* **30**, 357 (1997).
- [37] T. Schmiedl and U. Seifert, Efficiency of molecular motors at maximum power, *Europhysics Letters* **83**, 30005 (2008).
- [38] T. Lu, J. Zhou, N. Li, R. Yang, and B. Li, Inhomogeneous thermal conductivity enhances thermoelectric cooling, *AIP Advances* **4**, 124501.
- [39] J. Kaur and R. S. Johal, Thermoelectric generator at optimal power with external and internal irreversibilities, *Journal of Applied Physics* **126**, 125111.
- [40] H. Chen, Y. Huang, Z. Chen, and Y. Jiang, Performance analysis of the system integrating a molten carbonate fuel cell and a thermoelectric generator with inhomogeneous heat conduction, *Applied Thermal Engineering* **200**, 117729 (2022).
- [41] Y. Zhang, H. Liu, X. Zhou, Z. Hu, H. Wang, M. Kuang, J. Li, and H. Zhang, A novel photo-thermal-electric hybrid system comprising evacuated u-tube solar collector and inhomogeneous thermoelectric generator toward efficient and stable operation, *Energy* **292**, 130616 (2024).
- [42] J.-Z. Hu, B. Liu, J. Zhou, B. Li, and Y. Wang, Enhanced thermoelectric cooling performance with graded thermoelectric materials, *Japanese Journal of Applied Physics* **57**, 071801 (2018).

- [43] Y. Huang, Z. Chen, and H. Ding, Performance optimization of a two-stage parallel thermoelectric cooler with inhomogeneous electrical conductivity, *Applied Thermal Engineering* **192**, 116696 (2021).
- [44] Y. Apertet, H. Ouerdane, A. Michot, C. Goupil, and P. Lecoer, On the efficiency at maximum cooling power, *Europhysics Letters* **103**, 40001 (2013).
- [45] M. Chen, L. Rosendahl, I. Bach, T. Condra, and J. Pedersen, Irreversible transfer processes of thermoelectric generators, *American Journal of Physics* **75**, 815 (2007).
- [46] C. A. Domenicali, Irreversible thermodynamics of thermoelectricity, *Reviews of Modern Physics* **26**, 237 (1954).
- [47] R. S. Johal and R. Rai, Efficiency at optimal performance: A unified perspective based on coupled autonomous thermal machines, *Phys. Rev. E* **105**, 044145 (2022).
- [48] V. Singh and R. S. Johal, Feynman–Smoluchowski engine at high temperatures and the role of constraints, *Journal of Statistical Mechanics: Theory and Experiment* **2018**, 073205 (2018).
- [49] O. Höglblom and R. Andersson, Analysis of thermoelectric generator performance by use of simulations and experiments, *Journal of Electronic Materials* **43**, 2247 (2014).